Development of Erosion Hotspots for a Watershed

Tiao J. Chang, M.ASCE[1]; and Travis D. Bayes[2]

Abstract: The loss of topsoil in the United States has resulted in low crop yield, reduction of reservoir capacity, cost increase of water treatment, and detrimental effects on aquatic life and wildlife habitats. An initial step for taking conservation measures in any watershed is to identify locations where erosion protection measures are needed. Applying the Revised Universal Soil Loss Equation (RUSLE) and a geographic information system (GIS), this study attempts to locate the most erodible locations, namely erosion hotspots, for a watershed. Using GIS, the watershed is divided into 25 × 25-m grids and the RUSLE, including rainfall-runoff erosivity factor, soil erodibility factor, combined slope length and slope steepness factor, cover management factor, and support practice factor, is applied for the estimation of soil erosion potential for each grid cell. By ranking these grid values of erosion potential in a descending order, the top 1% and corresponding locations are defined as the erosion hot spots, which can be expressed in an erosion hotspot map. Applying this method to the Charles Mill Lake Watershed in Ohio, it is found that the erosion hotspots for the watershed under investigation are generally located in the areas of strip mine and cropland/pasture. **DOI: 10.1061/(ASCE)IR.1943-4774.0000648.** © *2013 American Society of Civil Engineers.*

CE Database subject headings: Soil erosion; Geographic information systems; Lakes; Watersheds; United States; Ohio.

Author keywords: Revised Universal Soil Loss Equation; Erosion hotspots; Cumulative histogram; Geographic information system; Soil erosion; Charles Mill Lake.

Introduction

Economic development has been at the expense of soil conservation in the past; indeed, crop yield has a direct correlation with soil loss. The economic impact of soil erosion in the United States costs the nation approximately $37.6 billion each year in productivity losses (Lang 2006). Soil erosion reduces transport ability in rivers and storage capacity of reservoirs, pollutes water supplies, and increases water treatment costs. Wildlife habitats are also greatly impacted by the sediment silting over fish beds as a result of erosion (Doerr et al. 2009). Suspended sediments in water result in low light infiltration and affect aquatic life in streams, lakes, reservoirs, and estuaries. Furthermore, sediment deposits reduce the capacities of channels and reservoirs and result in an overall increase in flooding.

Types of erosion generally take place in varied stages of an erosion process. The first type is raindrop erosion, in which the process starts as the raindrop falls at high velocities. Once a raindrop hits the soil surface, the soil is compacted under the raindrop and the detached soil particles are dispersed on the side. These soil particles can travel as far as 1 m vertically and up to 2 m horizontally down the slope (Chang et al. 2000, 2001). Minutes into a rainstorm, muddy water begins to infiltrate the soil and particles are filtered out by the soil. These particles, along with compaction of the soil and puddle, form a layer of soil that has a much lower infiltration rate than that of the soil alone. Consequently, this results in runoff rather than infiltration. In runoff, water carries soil particles that are splashed by the impact of raindrops. As the rain continues, raindrops pummel the soil into smaller and smaller particles. The smaller the particles, the faster they move as suspended materials of runoff. The raindrop splashes cause particle transport downhill and result in the next stage of erosion: sheet erosion, which is relatively slow and uniform. Over time, sheet erosion deteriorates to form small grooves or channels on the slope. This starts a new type of erosion called rill erosion. Small channels intensify the process of surface erosion because the channels created reduce friction and increase water velocity. The faster the velocity of runoff, the larger the particles it can carry; hence, the larger the runoff discharge, the more particles it can carry.

Next, gully erosion, an extremity of rill erosion, creates large channels including waterfalls. Large gorges allow large amounts of water to move swiftly and to consequently pick up more soil. Within gullies, freezing and thawing lead to slides and movements of large soil conglomerations and result in further erosion because of the explosion of loosened soil. When runoff reaches primary channel, the erosion process does not stop, but continues to the next form of erosion. Because channels tend to meander, water cuts into channel banks and erodes soils. Within the channel, shear stress attributable to the velocity gradient acts upon channel bed and banks, resulting in bank and bed erosions. The last stage of erosion is the deposition of soil particles, which usually happens in lakes, reservoirs, estuaries, and deltas. As the channel bed slope decreases, water velocity decreases, resulting in the settlement of soil particles. The more sediment deposited, the slower the water velocity because of the decrease of hydraulic gradient. The cycle intensifies the settling process.

Because of the complexity of erosion mechanics and processes in terms of soil detachment, transport, and settling, soil erosion has commonly been regarded and estimated on a large scale in a combination of four basic factors: topography, climate, soil characteristics, and land use (Romkens et al. 2002; McNulty et al. 1995; Goldman 1986). These four factors vary geographically in many watersheds. For instance, in the state of Ohio, the topography changes from the steep slope of the Appalachian foothills in the

[1]Professor, Civil Engineering Dept., Ohio Univ., Athens, OH 45701 (corresponding author). E-mail: chang@ohio.edu

[2]Environmental Engineer, Brown and Caldwell, 2674 Federated Blvd., Columbus, OH 43235.

Note. This manuscript was submitted on February 28, 2012; approved on June 21, 2013; published online on June 24, 2013. Discussion period open until May 1, 2014; separate discussions must be submitted for individual papers. This paper is part of the *Journal of Irrigation and Drainage Engineering*, Vol. 139, No. 12, December 1, 2013. © ASCE, ISSN 0733-9437/2013/12-1011-1017/$25.00.

Ohio River valley to the flat plains near the Great Lakes. The land use changes from urban to agricultural or forested and plays an important role in soil erosion. McIsaac et al. (1987) found a linear relationship between the soil loss and the sine value of the land slope. The steeper the slope, the faster the runoff; consequently, the soil loss increases with an increase of runoff. Wischmeier and Smith (1978) constructed a relationship between slope length and soil loss for erosion modeling. Foster et al. (1977) found a relationship between slope length and rill to interrill erosion. Rill to interrill erosion results in more quick soil erosion than sheet erosion, in which an increase of slope increases the soil loss. Experiments conducted by Gabriel (1999) concluded that soil loss increases with an increase of slope length.

Raindrops contribute more to sheet erosion than the sheet flow of runoff (Romkens et al. 2002; Morgan et al. 1998; Roose 1977). Soil losses during storms are directly proportional to storm parameters that can be combined as the product of the total storm energy and the maximum 30-min intensity (Wischmeier and Smith 1978). The storm energy is dependent on the amount of rainfall and its duration. On flat surfaces, water tends to pond to protect the soil from being eroded by the impact of raindrops; conversely, the opposite is true on steeper slopes (Mutchler 1970). The raindrop impact causes detachment of the soil, of which the splash is generally uniform in all directions on a flat surface. On steep slopes, more soil is splashed downhill. Morgan et al. (1998) found that 75% of the splash was in the downhill direction on a 10% slope. Other climatic factors, including temperature, wind, humidity, and solar radiation, also play role in soil erosion, but are difficult to be quantified for modeling (Schwab et al. 2002).

Barrow (1991) showed that loess soils tend to lose an extreme amount to erosion because of the type of soil's susceptibility to compaction and water logging when cultivated. Texture, organic matter content, structure, and permeability are the four basic soil characteristics that affect the erodibility of soil (Goldman 1986). The soil texture depends on the composition of the soil, or the weight percent of sand, silt, and clay. Silt and very fine sand are the soil particles that are the most vulnerable to erosion. In general, the higher the percentage of silt in a soil, the more erodible it is (Wischmeier and Smith 1978). Sand, as a larger particle, is more difficult to erode. However, once sand does erode, it will be deposited quickly. On the other hand, the clay particle can be carried for a relatively long distance before settling. Salt water increases the settling velocity by causing the clay particles to clump together, thus increasing the diameter of the particle. Organic matter helps to bind soil together, similar to clay, and increases permeability. The soil permeability increases the ability to absorb water during rainfall and reduce the amount of runoff. An increase of water absorption attracts plants to grow in the soil, helping to bind the soil and creating a better soil structure for resisting erosion. Furthermore, soil structure for the arrangement of soil particles is strongly related to erosion. The desired low erosive soil structure is a granular composition. Teixeira and Misra (1997) conducted experiments and demonstrated the importance of aggregate stability on the characteristics of soil erosivity.

Finally, land use affects the erodibility of soil because of the vegetation that reduces erosion by developing a canopy to intercept raindrops (Lopez et al. 1998; Long et al. 2006). In doing so, the raindrop loses energy to erode the soil. Roots of the vegetation increase the ground roughness, reducing runoff velocity and aggregating the soil, which increases porosity and reduces runoff. Furthermore, plants increase organic materials and use the moisture in the soil, through which organic materials bind particles of soil together, and the loss of soil moisture reduces runoff. In developing the erosion hotspots for a watershed, this study applies the Revised Universal Soil Loss Equation (RUSLE), which includes the preceding four essential parameters, combined slope length and slope steepness factor, rainfall-runoff erosivity factor, soil erodibility factor, and land cover management factor, for the estimation of soil erosion potential for each grid cell (Renard et al. 1997; Wischmeier and Smith 1978).

Development of Erosion Hotspots

By dividing the watershed into 25×25-m grids, the RUSLE is applied to each grid for estimating the soil erosion potential as follows:

$$A = R \times K \times L \times S \times C \times P \tag{1}$$

where A = soil loss potential for the grid in ton/acre/year, which is converted into kg/m^2/year for the development of erosion hotspots in this study; R = rainfall-runoff erosivity factor in hundreds of ft/tonf/inch/hour/acre/year; K = soil erodibility factor in (ton/acre/hour/hundreds of acre-ft/tonf/inch); L = dimensionless slope length factor; S = dimensionless slope steepness factor; C = dimensionless crop management factor; P = dimensionless support practice factor (Renard et al. 1997; Wischmeier and Smith 1978).

The rainfall and runoff erosivity factor, R, can be expressed by

$$R = EI_{30} \tag{2}$$

where E = storm energy; and I_{30} = maximum 30-min intensity. Local values can be derived from isoerodent maps based on the work of Wischmeier and Smith (1978). The isoerodent maps are developed by the USDA from the rainfall intensity duration frequency (IDF) data provided by the National Weather Service for the use in the United States. It can also be calculated for any location if the historical IDF data are known.

The soil erodibility factor, K, can be expressed by

$$K = \frac{2.1 \times 10^{-4}(12 - M_o)M^{1.14} + 3.25(S' - 2) + 2.5(P_s - 3)}{100} \tag{3}$$

where M_o = percentage of organic matter within the soil; S' = structure class value; P_s = permeability class value; and M is estimated by

$$M = A_s B_s \tag{4}$$

where A_s = percentage of soil whose diameter is between 0.002 and 0.1 mm; and B_s = percentage of soil whose diameter is between 0.1 and 2 mm.

The slope length factor, L, can be determined by the following equation:

$$L = \left(\frac{\lambda}{22.13}\right)^m \tag{5}$$

where λ = horizontal length in meters from the top of the slope to a point of concentration of the runoff (Renard et al. 1997); and m = variable slope length exponent, defined as follows:

$$m = \frac{\beta}{1 + \beta} \tag{6}$$

where β = rill erosion to interrill erosion, defined by the following equation (Foster et al. 1977):

Table 1. Land Uses and Associated Crop Management, C, Values

Land uses	C value
Residential	0.013
Commercial and services	0.003
Deciduous forest	0.001
Evergreen forest	0.005
Orchards, groves, vineyards	0.042
Reservoir	0.000
Industrial	0.003
Confined feeding operations	0.100
Strip mines, quarries, pits	0.100
Other urban or built up	0.013
Transportation, communication, utilities	0.013
Nonforested wetland	0.003
Cropland and pasture	0.050

$$\beta = \frac{\frac{\sin\theta}{0.0896}}{3.0(\sin\theta)^{0.8} + 0.56} \tag{7}$$

where θ = average land slope with the horizontal, in degrees (McCool et al. 1989).

The slope steepness factor, S, is defined by

$$S = \begin{cases} 10.8\sin\theta + 0.03 & \text{if } S \geq 9^\circ \\ 16.8\sin\theta - 0.50 & \text{if } S < 9^\circ \end{cases} \tag{8}$$

where θ = average land slope with the horizontal, in degrees (McCool et al. 1989). Variations of this equation and other equations can be used when cases arise of irregular slopes, such as a compound concave-convex slope (Foster and Wischmeier 1974).

The crop management factor, C, and the support practice factor, P, in the equation are provided with tables. The crop management factor depends on land use, canopy, surface cover, surface roughness, and soil moisture. Table 1 shows an example of land uses and associated crop management factors. The support practice factor describes agricultural areas in which varied methods such as crop rotation, reaping procedures, contouring, and terracing are used to reduce soil loss (Renard et al. 1997).

To estimate the parameters for the RUSLE for this study, Fig. 1 shows a flowchart for the process to result in the soil erosion potential for all the grid values. Based on the estimated grid values from the studied watershed, a cumulative histogram is constructed in which the 99th percentile value of the soil erosion potential soil is identified. Locations of which grid values are equal to or greater than the 99th percentile are defined as erosion hotspots. With this information, the erosion hotspot image can be produced to show their corresponding locations in the watershed for further analysis.

Applications and Results

The developed method was applied to the watershed of the Charles Mill Lake, which is located 7 km east of Mansfield, Ohio, in the Richland and Ashland counties, as shown in Fig. 2, which is produced based on free downloaded data (USGS 2013; *ArcGIS*). The watershed lies on the boundary of the glaciated portion of Ohio, in which the upper half of the watershed is flat and the lower half, toward the reservoir, is steep. The Black Fork Creek drains the entire watershed and discharges into the Charles Mill Lake in the northern end of the lake. The water from Charles Mill Lake ultimately discharges to the Ohio River via the Muskingum River. The dam holding Charles Mill Lake, constructed in 1935, has been operated by the U.S. Army Corps of Engineers for the purpose of

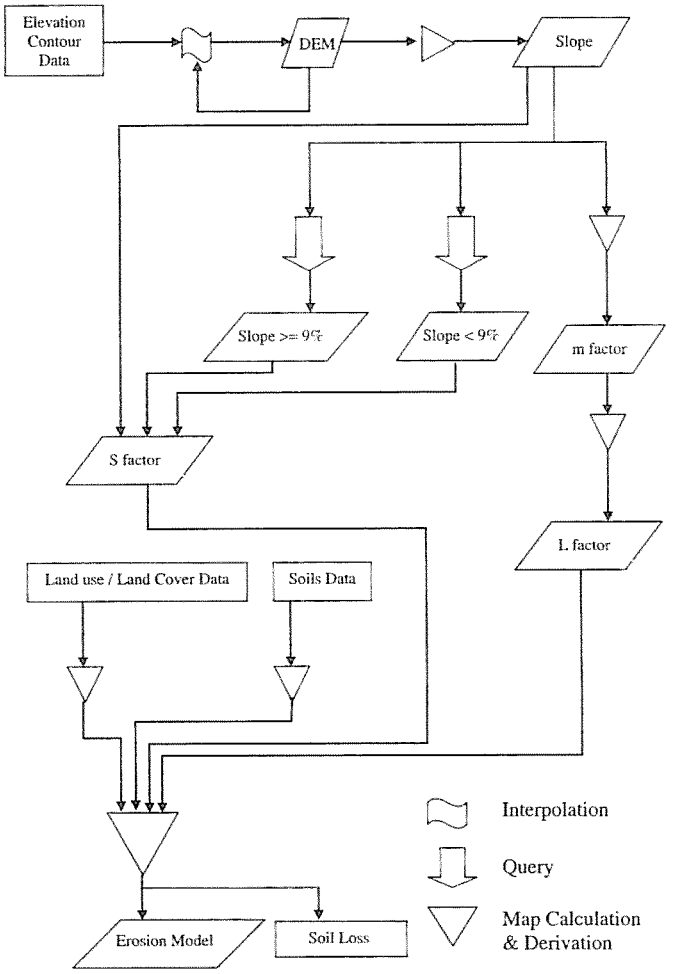

Fig. 1. Flowchart for the estimation of erosion potential

flood control. The Muskingum Watershed Conservancy District (MWCD) manages the lake, surrounding land, and recreational uses of the lake.

The watershed area of Charles Mill Lake is approximately 562 km^2. The watershed was digitized by using a hydrography and hypsography digital line graph (DLG) containing stream and contour data, in which USGS 1:24,000 hypsography DLGs are converted for the study. The hypsography data in vector format are converted into raster format, in which line vertices are converted into points (Chang et al. 2001). A grid theme is produced by using the tension model of the spline interpolator on point elevations. In general, smaller cell sizes produce better images, reducing error, but increase the computational burden (Molnár and Julien 1998). Mitra et al. (1998) found that cell sizes greater than 6 km^2 underestimate soil loss. In developing the erosion hotspots, this study uses a cell size of 625 m^2, in which the slope for each cell can easily be calculated by using the adjacent cells.

The amount of rainfall and runoff varies in the studied watershed, in which the rainfall and runoff erosivity factor for the RUSLE are determined by using the rainfall IDF data from the National Weather Service. The rainfall-runoff erosivity factor, R, can gradually change over a large area. The Charles Mill Lake watershed is approximately 562 km^2, which is relatively small compared to the variation of the rainfall-runoff erosivity factor. The variation over the watershed is less than 3%. Hence, an average value of erosivity estimated by using the IDF maps is used for the whole watershed. The average value used for the rainfall and runoff

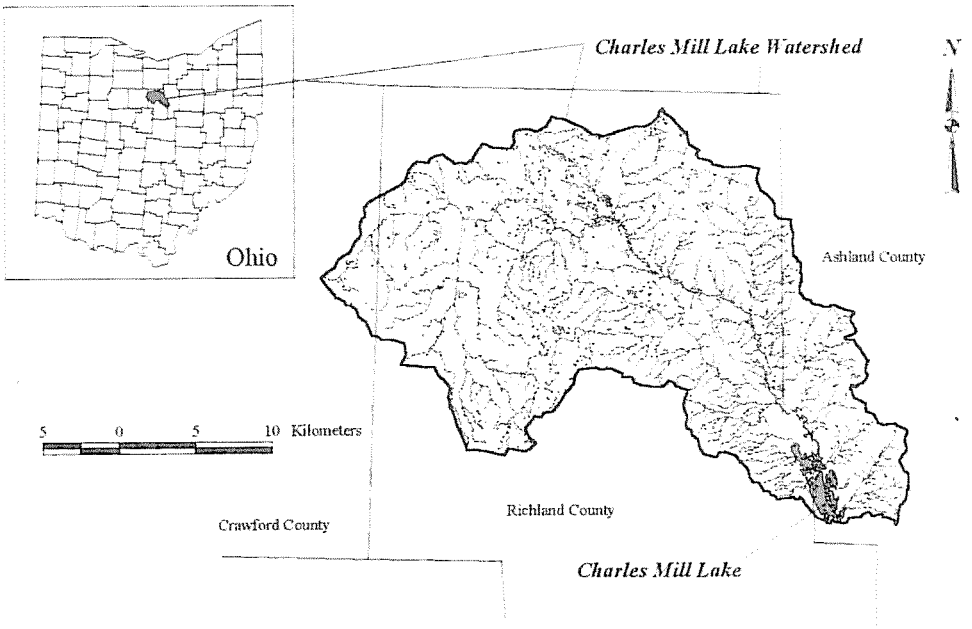

Fig. 2. Watershed of the Charles Mill Lake in Ohio (based on *ArcGIS* and USGS data)

erosivity factor is 1,889.22 MJ × mm/ha/h/year. If the watershed is significantly large, a surface of the rainfall and runoff erosivity factor can be interpolated for the watershed.

For the soil erodibility value that depends on the characteristics of soil, the digitized soil map used in this study contains 125 different soil types. Soil data include different soil parameters, such as grain size distributions, soil moisture, organic content, and permeability. Using these parameters, the soil erodibility value can be calculated by Eqs. (3) and (4). This database of soil parameters based on soil type is imported to join with the established spatial database, and converted into raster format with the same cell size as the other modeling parameters, to enable the analysis of erosion hotspots. It is found that the values of soil erodibility factor, K, have greater variations in the northwest section of the watershed and are relatively uniform toward the mouth of the reservoir in the southeast section. However, the soil erodibility factor is generally lower in the hilly southeast region of the watershed than in the flat area in the northwest region.

The calculation of the slope length, L, and slope steepness, S, factors relies on the digital elevation model (DEM) of the watershed, through which these factors are calculated by Eqs. (5) to (8) by using the GIS software (Chang et al. 2001). For the locations that have a land slope greater than or equal to 9°, the calculations of slope steepness are different from those less than 9°, as expressed in Eq. (8). It is found that the slope length factor, L, in the northwest section of the watershed tends to be lower than in the southeast region. Similarly, the slope steepness factor tends to increase toward the southeast section, near the lake. Furthermore, there are significant variations of slope steepness factors near the streams that drain throughout the whole watershed.

The crop management factor, C, is primarily developed by the tables available from the United States Environmental Protection Agency (USEPA) for the modeling process [National Land Cover Database (NLCD) 2006]. The digital spatially referenced land use and land cover data set are retrieved from the USEPA. The data set, originally stored geographically with the North American Datum in feet, is converted into Universal Transverse Mercator (UTM) Zone 17 with the same datum, but in meters, to be consistent with the geographically referenced mapping system used for this study. The crop management factor is established for each type of land use and attributed to the vector data set. They are converted into a raster format, similar to the soil erodibility factor. It is found that the variations of crop management factor in the watershed are relatively small, compared with other factors, as shown in Table 1. The support practice factor, P, is assumed to be equal to one because no significant method is adopted to protect against soil erosion in the studied watershed.

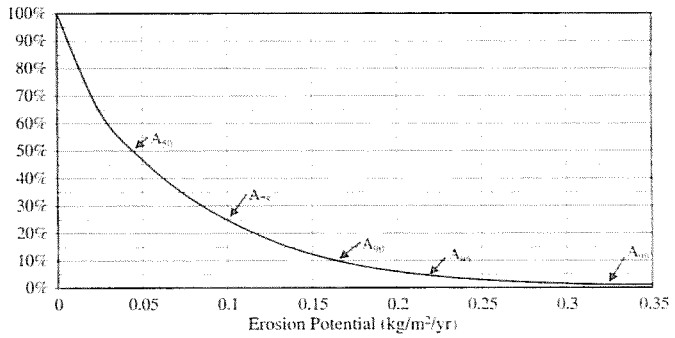

Fig. 3. Percentile values of erosion potentential in the studied watershed

Table 2. Percentile Values of Erosion Potential, Corresponding to Area Percentages

Percentile	Area (km^2)	Area (% of total)	Values ($kg/m^2/year$)
50th	276	50	>0.045
75th	139	75	>0.099
90th	54.7	90	>0.165
95th	27.5	95	>0.212
99th	5.5	99	>0.327

Table 3. Statistics of Erosion Potential According to Land Uses

Land uses	Cell count	Minimum ($kg/m^2/year$)	Mean ($kg/m^2/year$)	Maximum ($kg/m^2/year$)	Area (km^2)	Area (%)
Deciduous forest	65,401	0.0001	0.0266	0.309	41.50	7.38
Residential	41,534	0.0001	0.2104	2.0484	26.36	4.69
Commercial and services	3,894	0.0001	0.0299	0.3102	2.47	0.44
Evergreen forest	4,749	0.0001	0.1423	0.8248	3.01	0.54
Orchards	227	0.0576	0.5409	5.169	0.14	0.03
Industrial	2,313	0.0001	0.0322	0.3111	1.47	0.26
Confined feeding operations	28	0.1247	0.1835	0.3015	0.02	0.00
Strip mines	1,027	0.0001	2.6428	7.9955	0.65	0.12
Other urban or built up	1,491	0.0001	0.1806	0.7154	0.95	0.17
Transportation	12,367	0.0001	0.2911	2.7627	7.85	1.40
Nonforested wetland	3,861	0.0001	0.0537	0.4644	2.45	0.44
Cropland and pasture	748,701	0.0001	0.7909	25.8963	475.13	84.54
Total	885,593	—	—	—	562.00	100.00

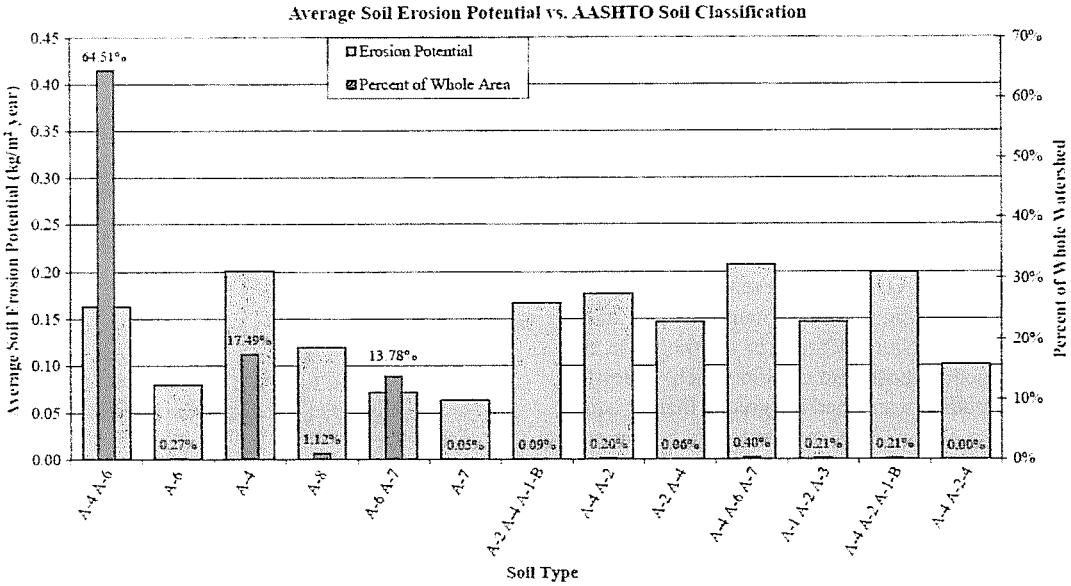

Fig. 4. Erosion potential accoding to soil types in the studied watershed

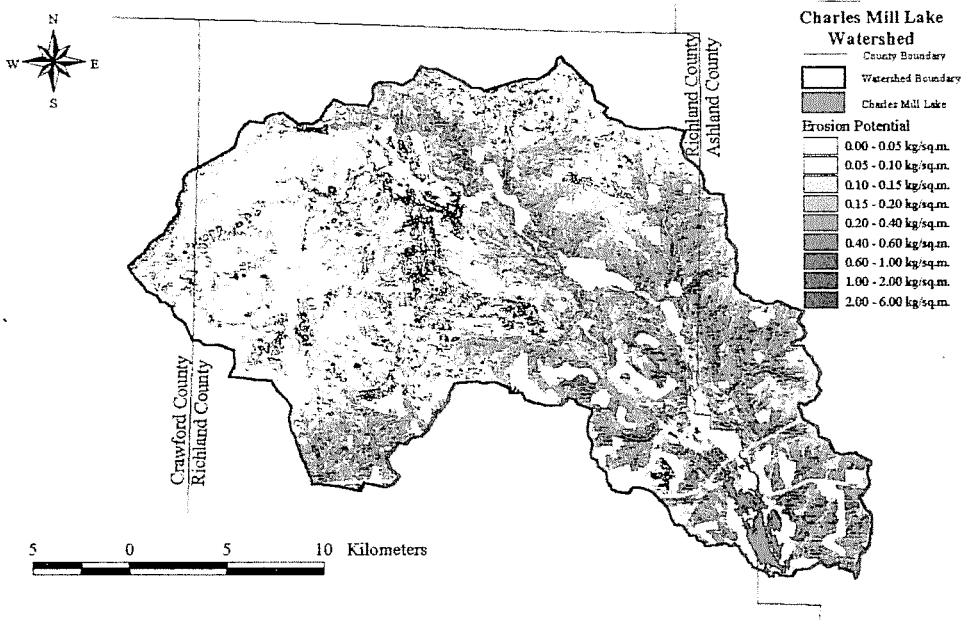

Fig. 5. Map of erosion hotspots in the Charles Mill Lake watershed (based on *ArcGIS* and USGS data)

Based on Eq. (1), the erosion potential values in kg/m^2/year for all of the 25 × 25-m grid cells in the studied watershed are obtained and ranked in descending order, through which the percentile values can be obtained from the cumulative histogram, as shown in Fig. 3. Table 2 lists the 50th to 99th percentiles of the erosion potential values corresponding to the area percentages of the watershed. The 99th percentile erosion potential is found to be 0.327 kg/m^2/year, but there are regions in which the values are as large as 5.80 kg/m^2/year. It is also found that the values of erosion potential in the east section of the watershed, particularly the southeast region, are much greater than those in the west.

Land uses ranging from residential area to strip mine in the watershed significantly affect the erosion potential. By comparing the common attributes of land use and the potential for erosion, Table 3 shows the statistics of grid values of erosion potential according to land uses in the watershed and the percentages of land uses in the watershed. It is found that the largest grid value of erosion potential occurs in the cropland/pasture, but the largest mean value is from strip mines. The former makes up 84.5% of the total watershed and has the second highest average erosion potential, next to strip mines, which represent 0.1% of the area.

Based on the classification of soil types by AASHTO, it is found that A-4 A-6 was the dominant soil type, making up 64.51% of the watershed, as shown in Fig. 4; combining A-4 A-6 with the other two types, A-4 and A-6 A-7, this represents 95.8% of the watershed. It is also found that the erosion potential values of all soil types in the watershed are relatively uniform. Furthermore, the erosion hotspots are defined as those grid cells in which values for erosion potential for the studied watershed are greater than or equal to that of 99th percentile, i.e., 0.327 kg/m^2/year. Fig. 5 is an erosion hotspot image that shows the spatial distribution of erosion potential in the studied watershed based on free downloaded data (USGS 2013; *ArcGIS*).

Conclusions

The proposed method seems capable of identifying the locations of erosion hotspots, which are most vulnerable to erosion, and providing further analysis to relate these locations to potential problems. For the watershed in this study, it is found that the most vulnerable land uses are strip mines and cropland/pasture. Furthermore, it is also found that the soil erodibility has greater variations in the northwest section than in the southeast section toward the mouth of the reservoir; however, the erodibility factor is generally lower in the southeast hilly region of the watershed than in the flat area in the northwest region. On the other hand, erosion potential according to the soil types in the studied watershed are relatively uniform, in which three major types of soil make up 95.8% of the watershed: A-4, A-7, A-4, and A-6 A-7, based on the AASHTO classification.

Acknowledgments

The support provided by the Muskingum Watershed Conservancy District in Ohio is gratefully acknowledged. The authors also want to thank the Huntington District, U.S. Army Corps of Engineers for the assistance for the study. Assistance for preparing the manuscript provided by Ms. Hong Zhou, Research Assistant, Civil Engineering Department, Ohio University is appreciated.

References

ArcGIS [Computer software]. Environmental Systems Research Institute (ESRI), Redlands, CA.

Barrow, C. J. (1991). *Land degradation: Development and breakdown of terrestrial environments*, University Press, Cambridge, MA.

Chang, T. J., Bartrand, T. A., and Germain, R. (2001). "Spatial variations of water loss during drought: A GIS case study." *J. Am. Water Resour. Assoc.*, 37(1), 115–123.

Chang, T. J., Bayes, T. D., and McKeever, S. (2000). "Selection of wetland sites for reservoir dredging materials using GIS." *Proc., Options for Dredged Material Disposal Management*, MIT Sea Grant Program Press, Cambridge, MA.

Doerr, S. H., Woods, S. W., Martin, D. A., and Casimiro, M. (2009). "Natural background soil water repellency in conifer forests of northwestern USA." *J. Hydrol.*, 371(1–4), 12–21.

Foster, G. R., Meyer, L. D., and Onstad, C. A. (1977). "A runoff erosivity factor and variable slope length exponents for soil loss estimates." *Trans. ASAE*, 20(4), 683–687.

Foster, G. R., and Wischmeier, W. H. (1974). "Evaluating irregular slopes for soil loss prediction." *Trans. ASAE*, 17, 305–309.

Gabriel, D. (1999). "The effect of slope length on the amount and size distribution of eroded silt loam soils: Short slope laboratory experiments on interrill erosion." *Geomorphol.*, 28(1–2), 169–172.

Goldman, S. (1986). *Erosion and sediment control handbook*, McGraw-Hill, New York, 5.2–5.15.

Lang, S. S. (2006). "Slow, insidious soil erosion threatens human health and welfare as well as environment." *Chronicle Online*, Cornell University, Ithaca, NY.

Long, H. L., et al. (2006). "Land use and soil erosion in the upper reaches of the Yangtze River." *Land Degrad. Develop.*, 17(6), 589–603.

Lopez, T. M., Aide, T. M., and Scatena, F. N. (1998). "The effect of land use on soil erosion in Guadiana Watershed in Puerto Rico." *Caribbean J. Sci.*, 34(3–4), 298–307.

McCool, D. K., Foster, G. R., Mutchler, C. K., and Meyer, L. D. (1989). "Revised slope length factor for the Universal Soil Loss Equation." *Trans. ASAE*, 32, 1571–1576.

McIsaac, G. G., Mitchell, J. K., and Hirschi, M. C. (1987). "Slope steepness effects on soil loss from disturbed lands." *Trans. Am. Soc. Agric. Eng.*, 30(4), 1005–1013.

McNulty, S., Swift, L., Hayes, J., and Clingapeel, A. (1995). "Predicting watershed erosion protection and overland sediment transport using GIS." *Proc., Int. Erosion Control Assoc. (IECA)*, International Erosion Control Association, Denver, CO, 397–406.

Mitra, B., Scott, H. D., Dixon, J. C., and McKimmey, J. M. (1998). "Applications of fuzzy logic to the prediction of soil erosion in a large watershed." *Geoderma*, 86(3–4), 183–209.

Molnár, D. K., and Julien, P. Y. (1998). "Estimation of upland erosion using GIS." *Comput. Geosci.*, 24(2), 183–192.

Morgan, R. P. C., et al. (1998). "The European soil erosion model: A dynamic approach for predicting sediment transport from field and small catchment." *Earth Surf. Processes Landforms*, 23(6), 527–544.

Mutchler, C. K. (1970). "Splash of a waterdrop at terminal velocity." *Sci.*, 169(3952), 1311–1312.

National Land Cover Database (NLCD). (2006). *A database for national land cover maintained by Multi-Resolution Land Characteristics Consortium (MRLC)*, USGS, Sioux Falls, SD.

Renard, K. G., Foster, G. R., Weesies, G. A., McCool, D. K., and Yoder, D. C. (1997). *Predicting soil erosion by water: A guide for conservation planning with the Revised Universal Soil Loss Equation (RUSLE)*, USDA, Washington, DC.

Romkens, M. J. M., Helming, K., and Prasad, S. N. (2002). "Soil erosion under different rainfall intensities, surface roughness, and soil water regimes." *Catena*, 46(2–3), 103–123.

Roose, E. J. (1997). *Use of the Universal Soil Loss Equation to predict erosion in West Africa, soil erosion: Prediction and control*, Soil Conservation Society of America, Anheny, IA, 60–74.

Schwab, G. O., Fangmeier, D. D., Elliot, W. J., and Frevert, R. K. (2002). *Soil and water management systems*. Wiley, New York.
Teixeira, P. C., and Misra, R. K. (1997). "Erosin and sediment characteristics of cultivated forest soils as affected by the mechanical stability of aggregates." *Cantena*, 30(2–3), 119–134.
USGS. (2013). "United States Geological Survey (USGS) national map site for the data." (http://nationalmap.gov/viewer.html).
Wischmeier, W. H., and Smith, D. D. (1978). "Predicting rainfall erosion losses—A guide to conservation planning." *Handbook No. 537*, U.S. Dept. of Agriculture, Washington, DC.